SLAC-PUB-1077
(TH) and (EXP)
July 1972

MEASUREMENT OF THE INCLUSIVE ELECTROPRODUCTION OF HADRONS*

J. T. Dakin, G. J. Feldman, W. L. Lakin**,
F. Martin, M. L. Perl, E. W. Petraske†, W. T. Toner‡

Stanford Linear Accelerator Center
Stanford University, Stanford, California 94305

ABSTRACT

The electroproduction of hadrons was studied with a wide-aperture spectrometer. Inclusive data are presented for the electron-scattering region $-.5 > q^2 > -2.5$ $(\mathrm{GeV}/c)^2$, $4 < \nu < 14$ GeV. Distributions of the electroproduced hadrons in the 3 inclusive variables φ, $p_\perp^2$ and x are studied in the region $x > 0$. A striking difference from photoproduction is observed in the excess of positive to negative hadrons at high x and high q^2.

* Work supported by the U. S. Atomic Energy Commission

** Present address: Birmingham Radiation Centre, University of Birmingham, P.O. Box 363, Birmingham B15 2TT, England

† Present address: Vanderbilt University, Nashville, Tennessee 37203

‡ Present address: Rutherford High Energy Laboratory, Chilton, Didcot, Berkshire, England

(Submitted to Phys. Rev. Letters. An expanded version of this paper is available as SLAC-PUB-1074, which was submitted to the XVI International Conference on High Energy Physics, Batavia, Illinois, Sept. 6-13, 1972.)

With the recent work in deep inelastic electron-nucleon scattering and its subsequent theoretical interpretations, there has been increasing interest in the hadronic final states produced in such interactions[1]. Here we report some preliminary results on the inclusive electroproduction of hadrons.

In this experiment, we detected in coincidence an electron scattered from a hydrogen target and one or more electroproduced hadrons. Taking each combination of a scattered electron and an electroproduced hadron as an independent inclusive event, the cross section is a function of six variables. Three of them are determined by the electron system: E, the incident electron energy in the laboratory (fixed at 19.5 GeV for all of our data); q^2, the invariant momentum transfer squared to the scattered electron; and ν, the electron energy loss in the laboratory. The remaining three, which concern the detected hadron, are calculated relative to the direction of the electron three-momentum transfer: x, the ratio of the longitudinal momentum in the virtual photoproduction center of mass system to the maximum possible; p_1^2, the transverse momentum squared; and φ, the hadron azimuthal angle.

Virtual photoproduction cross sections can be derived from experimental cross sections by

$$\frac{d\sigma}{dq^2\, d\nu\, d^3p} = \Gamma\,(E,\, q^2,\, \nu) \quad \frac{d\sigma(q^2,\, \nu)}{d^3p} \qquad (1)$$

where the Γ function contains the electrodynamic factors describing the electron-photon vertex. We will report here ratios of differential virtual photon cross sections to the total virtual photon cross section. These ratios are derived directly from our data since we had no require-

ment for a hadron in our trigger.

The differential cross sections will be given in a Lorentz invariant form:

$$E \frac{d\sigma(q^2,\nu)}{d^3p} = 2 \frac{E^*}{p^*_{max}} \frac{d\sigma(q^2,\nu)}{dx\, dp_\perp^2\, d\varphi} , \qquad (2)$$

where E^* is the energy of the hadron in the center of mass and p^*_{max} is the maximum possible center of mass momentum.

The experimental apparatus consisted of a 19.5 GeV electron beam incident on a target, and a large aperture spectrometer to detect a large fraction of the forward final state particles with lab momenta greater than ~ 1 GeV/c. These elements are shown in Fig. 1.

The electron beam contained typically 10^4 e^- per 1.5 μsec long SLAC pulse. The momentum band was 0.2% at 19.5 GeV/c. The target was 4 cm long, and was filled with either hydrogen or deuterium. Only the hydrogen data is reported here.

The spectrometer magnet had a field integral of 17 k Gauss-meters. The unscattered beam and the forward electromagnetic backgrounds passed through the magnet in a field-free region created by a cylindrical superconducting tube[2]. Beyond the magnet were two optical spark chambers separated by 1.7 m. Each chamber had a mirror system which allowed tracks to be seen in three views.

The apparatus was triggered on the detection of a scattered electron by a hodoscope of 20 scintillation counters and 11 shower counters[3] behind the second spark chamber. The shower counter thresholds were set to ~ 5 GeV.

The pictures taken with hydrogen in the target were scanned and

measured and the particle trajectories were reconstructed in space using two independent systems. The first was Hummingbird II, a flying spot digitizer, with which we measured all tracks in all pictures[4]. The second was a conventional hand system with which we measured only events with 2 or more tracks in 20% of the pictures.

Each system had only ~ 50% efficiency for fully reconstructing events with 2 or more tracks, largely because of confusion introduced by spurious tracks. We have not as yet thoroughly studied biases introduced by these inefficiencies. Biases, if any, should be different for the two systems since the Hummingbird identifies tracks on the basis of the stereo reconstruction while the hand system relies on pattern recognition of spark densities. We have verified that both systems give the same physics results within statistics. The data reported here are solely from the Hummingbird system.

In each reconstructed picture, the electron was identified by matching the positions and momenta of tracks to the position and pulse height of the shower counter which triggered the event. The remaining tracks which were consistent with the scintillator hodoscope pattern for an event were assumed to be hadrons. In a picture in which an electron was identified, if a hadron was present it was identified with $(70 \pm 10)\%$ efficiency. The r.m.s. momentum resolution was 2% at 10 GeV.

We have no means of distinguishing pions, kaons, and protons from each other. Hence we will refer only to positively and negatively charged hadrons and use the symbol "h" to describe them. In computing x, each h is assumed to be a π.

To prepare the physics distribution each event was weighted inver-

sely as its detection probability, a function of q^2, ν, φ, $p_\perp^2$, x, and h charge. To study the dependence of the data on one of these variables, we summed over some range of the other five variables. When such summations passed over small regions of zero acceptance, corrections were made for the missing events.

The cross sections thus obtained were normalized to the total virtual photoproduction cross section in the same q^2, ν region ($\sigma(q^2, \nu)$), obtained from the data. The data presented here are 6244 events from the region $4 < \nu < 14$ GeV, $-0.5 > q^2 > -2.5(\mathrm{GeV}/c)^2$, the region where the virtual photon direction is well within the geometric acceptance.

We have made a preliminary study of radiative and spatial resolution effects and have found that they produce no noticeable changes in the shapes of the $p_\perp^2$ and x distributions at the statistical level of this experiment. No corrections for these effects have been made in the data presented here.

The errors given in figures in this report represent statistical errors only. There is in addition a possible 15% error due primarily to uncertainty in the level of Hummingbird efficiency.

We observe no significant φ dependence in the data, although the negative hadron data are consistent with π^- photoproduction measurements which show transverse polarization effects at high x.[5] As an aid in extracting $p_\perp^2$ and x distributions, the subsequent analysis assumed that the φ distribution was flat.

The $p_\perp^2$ dependence of the data in the range $0 < p_\perp^2 < .7$ $(\mathrm{GeV}/c)^2$ was studied as a function of q^2, ν, x, and h charge and was found not to depend on any of these variables in a statistically significant way. The

data are fit well with a function of the form A $e^{-bp_T^2}$ with b = 4.7 ± .5 $(GeV/c)^{-2}$. We have extracted a value of b = 5.9 ± .2 $(GeV/c)^{-2}$ for the same x and ν (E_γ) range from the π^- photoproduction data[5].

The dependence of the invariant cross section on x is shown in Fig. 2 for positive and negative hadrons. The curve for negative hadrons agrees with the analogous photoproduction[5] curve at low x, but falls a factor of 2 to 3 below it at higher x. The slow fall of the photoproduction distribution at moderate x values is due largely to the production of rho mesons. If proportionally fewer rho mesons were electroproduced than photoproduced, one would expect the distribution to fall more sharply.

Figure 3 shows the ratio of the invariant cross sections for positive hadrons to those for negative hadrons as a function of x. There is a striking increase in the ratio as x increases.

There are no published photoproduction data for this ratio. However, from available information we estimate the photoproduction ratio to be 1.20 ± .10 throughout this x range. The SLAC-Berkeley-Tufts bubble chamber data[6] give a ratio between 1.00 and 1.10 in this range. These data exclude two classes of events, one-prong events and visible strange particle production, which together compose ~ 15% of the cross section and which predominately yield positive hadrons. The ratio of 1.20 ± .10 is also consistent with low p_T^2 SLAC spectrometer data[7]. Our data appear to approach the photoproduction value as $x \to 0$.

In Fig. 4 we show the charge ratio as a function of q^2 for two ranges of x. The ratio increases markedly as $|q^2|$ increases, and appears to approach the photoproduction value as $q^2 \to 0$.

It is not clear whether the effect shown in Fig. 4 is a function of

q^2 or $\omega = 2M\nu/q^2$ (or both). There is some evidence in the data that at fixed q^2 the charge ratio is largest at small ω, but we have been unable to establish this on a statistically significant level for all of our data.

We consider these data to be significant and surprising. As $|q^2|$ increases or as ω decreases, by some mechanism, part of the charge of the proton is being projected forward. We note that quark-parton models can yield a charge ratio as large as 8 at small ω and large x.[8]

We wish to acknowledge the technical support contributed by numerous SLAC groups, particularly the cooperation from Steve St. Lorant and the Low Temperature group, and John Brown and the Data Analysis group. Byron Dieterle and Benson T. Chertok provided valuable assistance in the early stages of the experiment.

REFERENCES

1. The current status of these topics is summarized in talks by H. Kendall, K. Berkelman and J. Bjorken in International Symposium On Electron and Photon Interactions at High Energies, Cornell University, Ithaca, N. Y. (1971), edited by N. B. Mistry.
2. F. Martin, S. J. St. Lorant and W. T. Toner, Nucl. Instr. and Methods (to be published).
3. W. L. Lakin, E. W. Petraske, W. T. Toner, Nucl. Instr. and Methods (to be published).
4. J. L. Brown, Stanford Linear Accelerator Center report no. SLAC-PUB-752 (1970).
5. K. C. Moffeit, J. Ballam, G. B. Chadwick, M. Della-Negra,

R. Gearhart, J. J. Murray, P. Seyboth, C. K. Sinclair, I. O. Skillicorn, H. Spitzer, G. Wolf, H. H. Bingham, W. B. Fretter, W. J. Podolsky, M. S. Rabin, A. H. Rosenfeld, R. Windmolders, G. P. Yost and R. H. Milburn, Phys. Rev. D5, 1603 (1972).

6. K. C. Moffeit (private communication).

7. A. M. Boyarski, D. Coward, S. Ecklund, B. Richter, D. Sherden, R. Siemann and C. Sinclair, Contribution to the International Symposium On Electron and Photon Interactions at High Energy, Ithaca, New York (1971) and private communication.

8. For example, see C.F.A. Pantin, University of Cambridge, preprint no. DAMTP 7219 (1972).

FIGURE CAPTIONS

1. Schematic view of the apparatus.
2. Dependence of the invariant cross section on x for $-.5 > q^2 > -2.5$ $(\text{GeV}/c)^2$, $4 < \nu$ 14 GeV. A line representing the data in π^- photoproduction (Ref. 5) is included.
3. The ratio of the invariant cross section for positive to negative hadrons at each x for $-.5 > q^2 > -2.5$ $(\text{GeV}/c)^2$ and $4 < \nu < 14$ (GeV).
4. The ratios of the invariant cross section for positive to negative hadrons at each q^2 for two different x ranges. A point at $q^2 = 0$ from photoproduction (Refs. 6 and 7) is included.

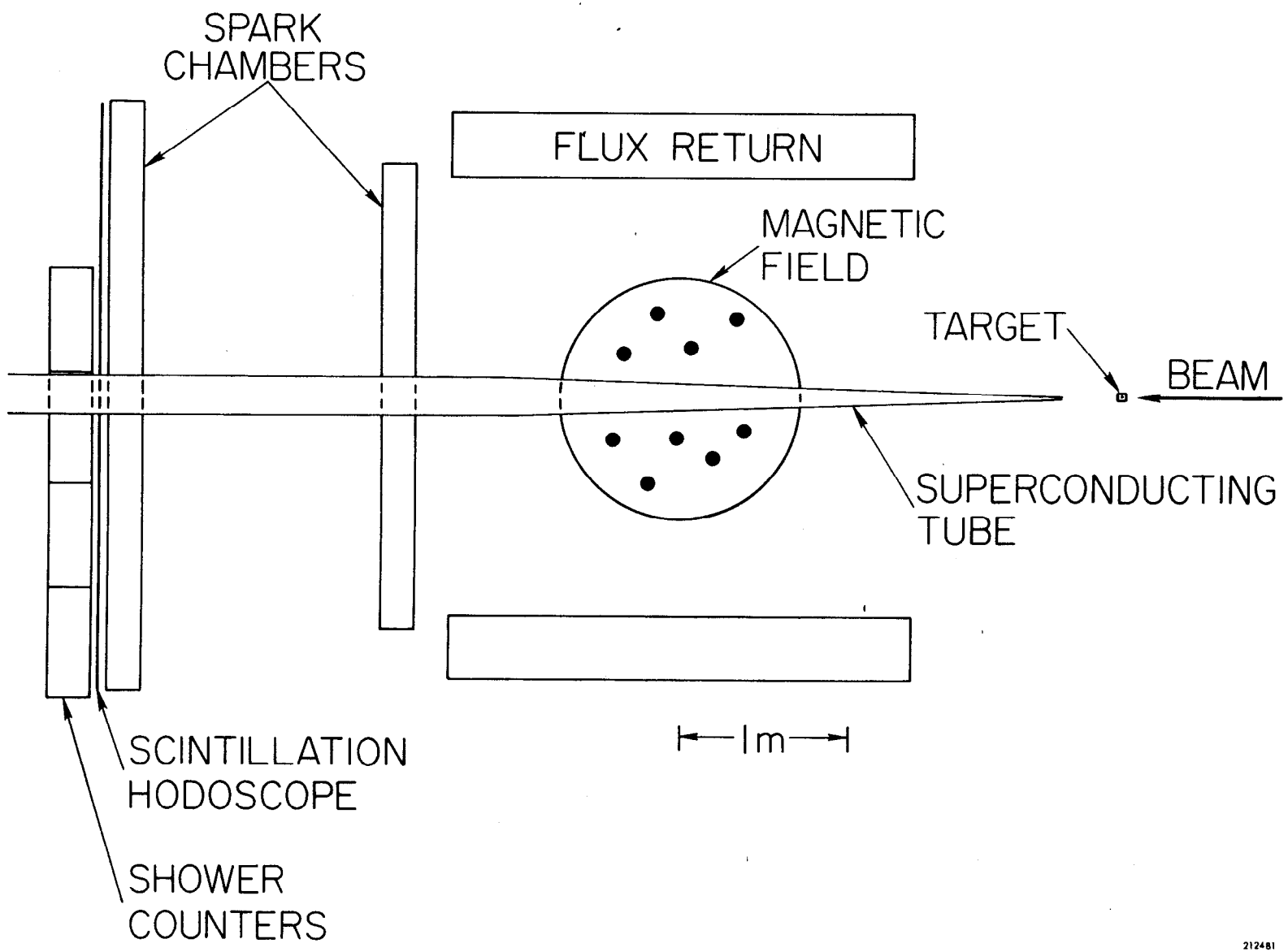
SPARK
CHAMBERS
FLUX RETURN
MAGNETIC
FIELD
TARGET
BEAM
SUPERCONDUCTING
TUBE
SCINTILLATION
HODOSCOPE
SHOWER
COUNTERS
1m
212481

Fig. 1

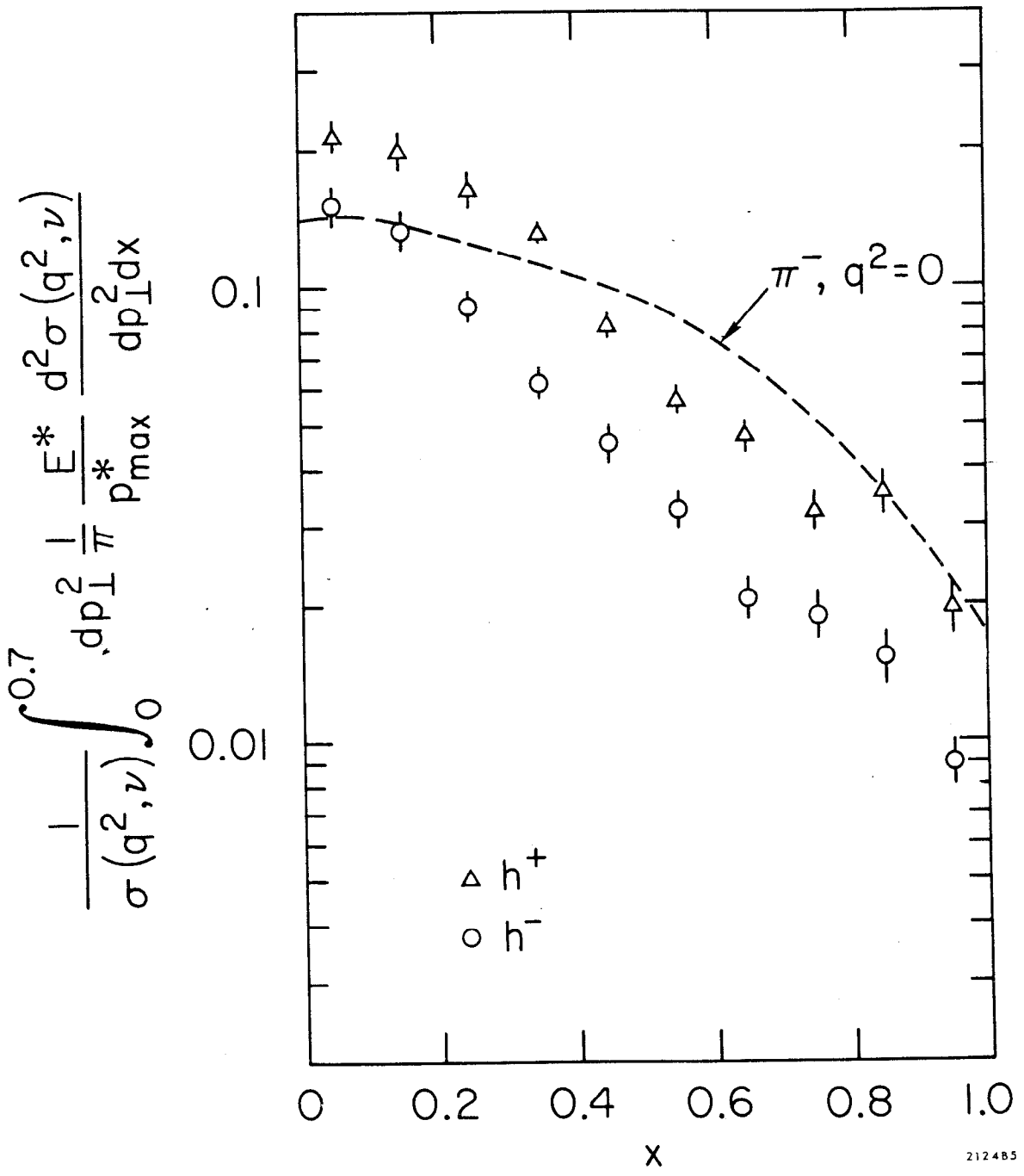
$\frac{1}{\sigma(q^2,\nu)}\int_0^{0.7} dp_T^2 \frac{1}{\pi}\frac{E^*}{p^*_{max}}\frac{d^2\sigma(q^2,\nu)}{dp_T^2 dx}$
0.1
0.01
π^-, $q^2=0$
h^+
h^-
0
0.2
0.4
0.6
0.8
1.0
x
2124B5

FIG. 2

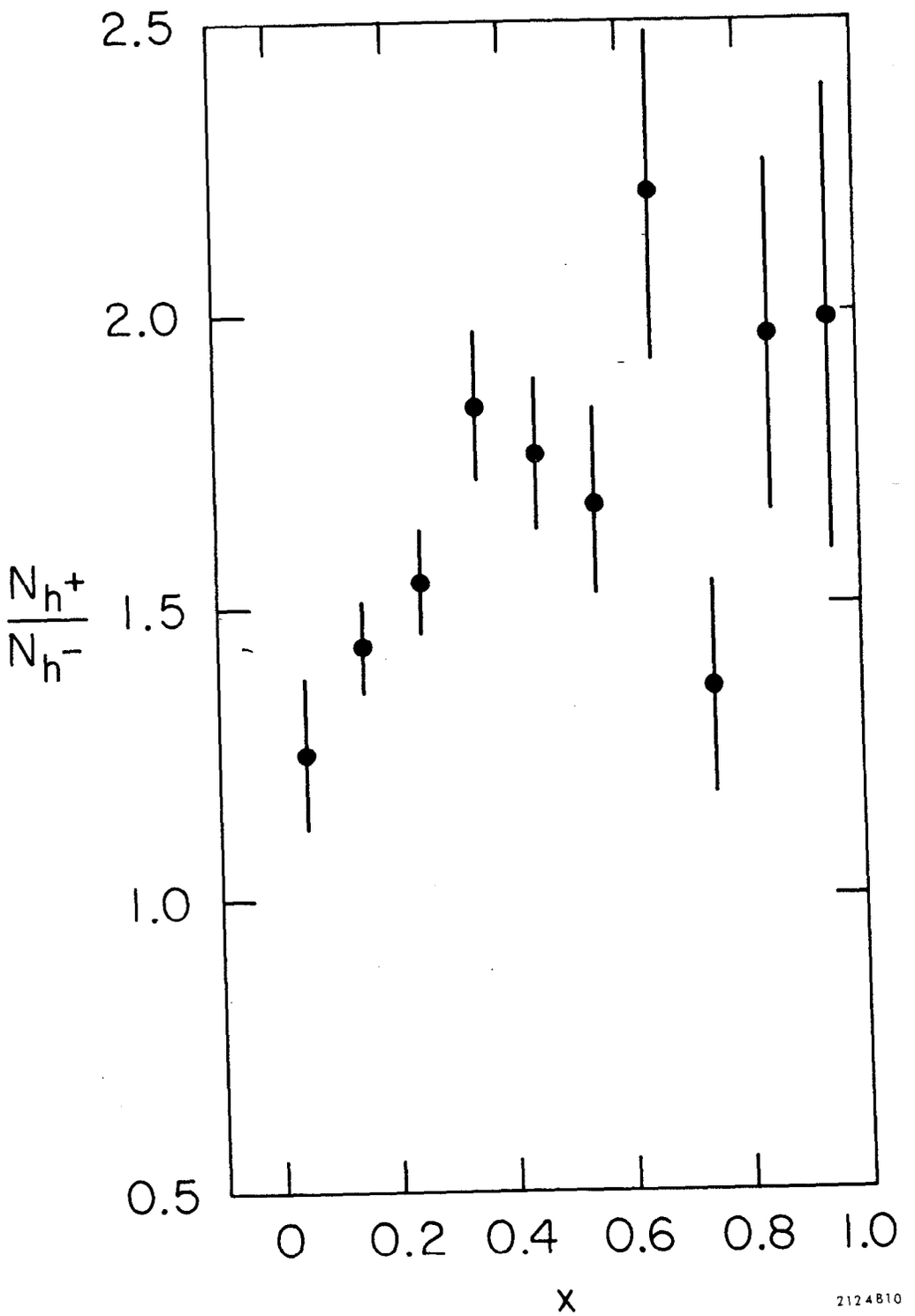

FIG. 3

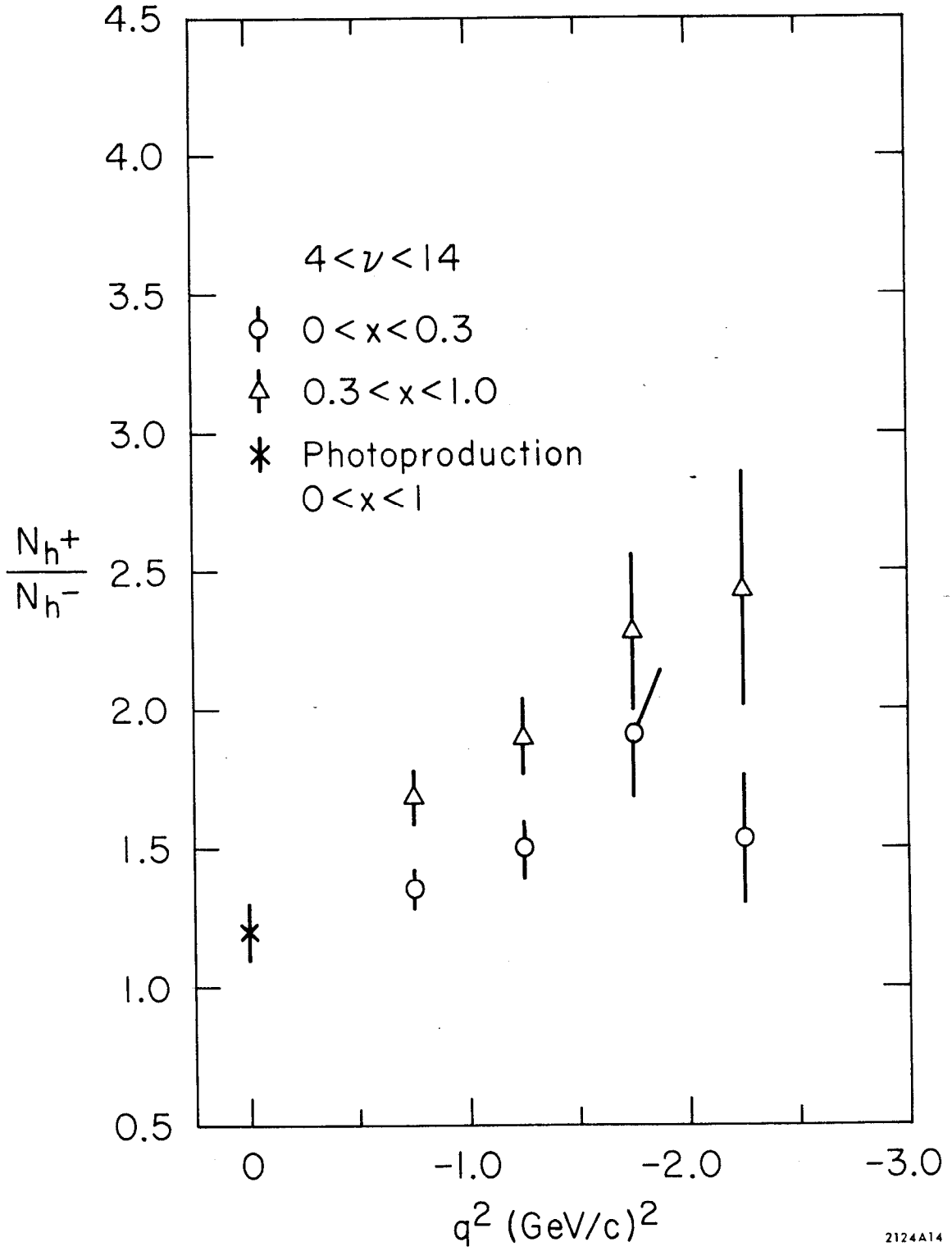
4.5
4.0
3.5
3.0
2.5
2.0
1.5
1.0
0.5
$\frac{N_{h^+}}{N_{h^-}}$
$4<\nu<14$
$0<x<0.3$
$0.3<x<1.0$
Photoproduction
$0<x<1$
0
-1.0
-2.0
-3.0
q^2 (GeV/c)^2
2124A14

FIG. 4